Measurement of the decay $B \to KK\ell\nu$

Matic Lubej

Ljubljana, 2018

Changelog

Contents

Page

1 Introduction **2**

2 Data and MC **3**

3 Event reconstruction **4**
3.1 Final state particles selection 4
3.2 Combination of FSP particles 11
3.3 Rest of event clean-up 13
3.4 Loose neutrino reconstruction 14
3.5 q^2 calculation 15

4 Rest of event clean-up **16**
4.1 Setting up the MVA 16
4.2 Clusters clean-up 17
4.2.1 π^0 MVA training 17
4.2.2 γ MVA training 18
4.2.3 Clusters clean-up optimization 19
4.3 Tracks clean-up 19
4.4 Selection after clean-up 19

1 Introduction

test

2 Data and MC

test

3 Event reconstruction

In this chapter the procedure for event reconstruction of the decay Decay is shown, starting from final state particle selection and combining particles up the chain all the way to the B meson.

3.1 Final state particles selection

Since the neutrino escapes detection, we can only reconstruct the charged tracks of our decay, which are the two kaons (K) and the light lepton, which is the electron (e) or muon (μ). These are some of the particles which are commonly referred to as final state particles (FSP). Final state particles have a long lifetime and are usually the particles that we detect when they interact with the material in the detector.

It is important to limit our selection of FSP particles in order to cut down the number of particle combinations and to reduce computation time and file sizes.

Leptons

Figures 3.1 and 3.2 show the impact parameters d_0 and z_0, the momentum in $\Upsilon(4S)$ center-of-mass system (CMS), and the PID information for true and fake electrons and muons, where an extra category for true electrons/muons from the signal decay is shown.

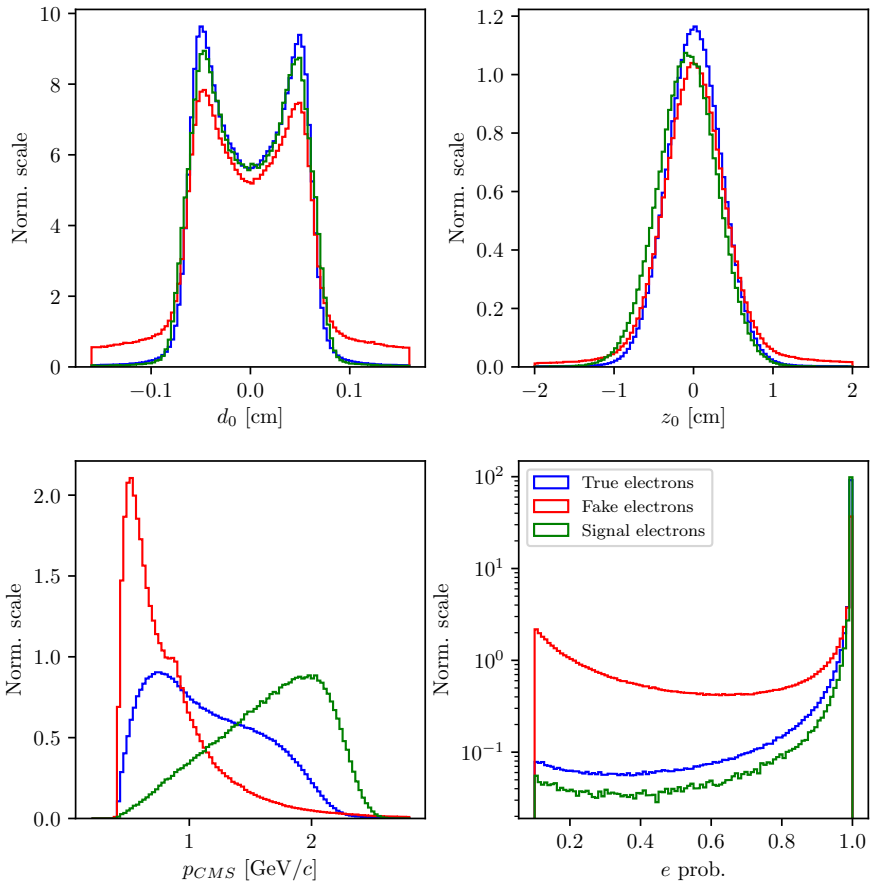

Figure 3.1: Normalized properties of true (blue), fake (red) and true electrons (green) from signal decay

.

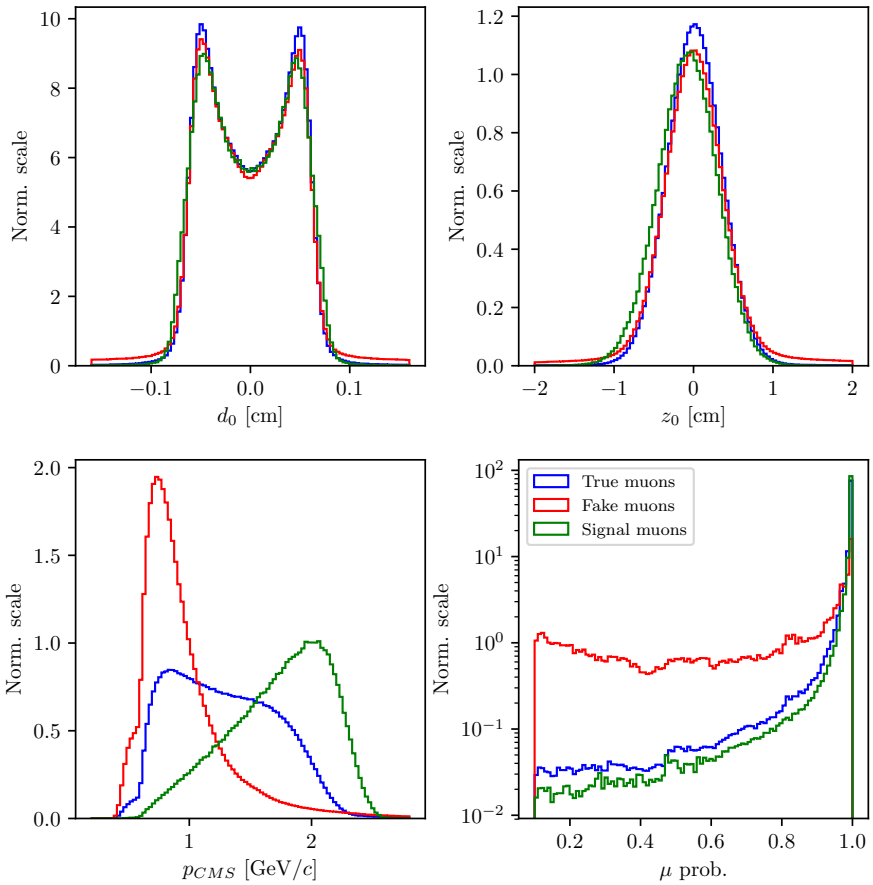

Figure 3.2: Normalized properties of true (blue), fake (red) and true muons (green) from signal decay

.

Based on the first plots, we can define a set of cuts:

- $|d_0| < 0.1$ cm,
- $|z_0| < 1.5$ cm,
- $p_{LAB} > 0.6$ GeV/c and $p_{CMS} \in [0.4, 2.6]$ GeV/c for electrons,
- $p_{CMS} \in [0.6, 2.6]$ GeV/c for muons,

where the p_{LAB} momentum cut for the electron case is chosen to discard a region with a sharp jump, which is assumed to come from sources like hard coded values in Belle software.

With this selection we can now determine the optimal PID cuts for electrons and muons, where we optimize with the standard definition of *figure of merit* (FOM), shown in

Figures 3.3 and 3.4. The cuts are optimized in steps of 0.1, since we will later need to apply the PID correction factors, which are only available for cuts of these values.

$$FOM = \frac{S}{\sqrt{S+B}}, \tag{3.1}$$

where S represents number of signal and B the number of background candidates.

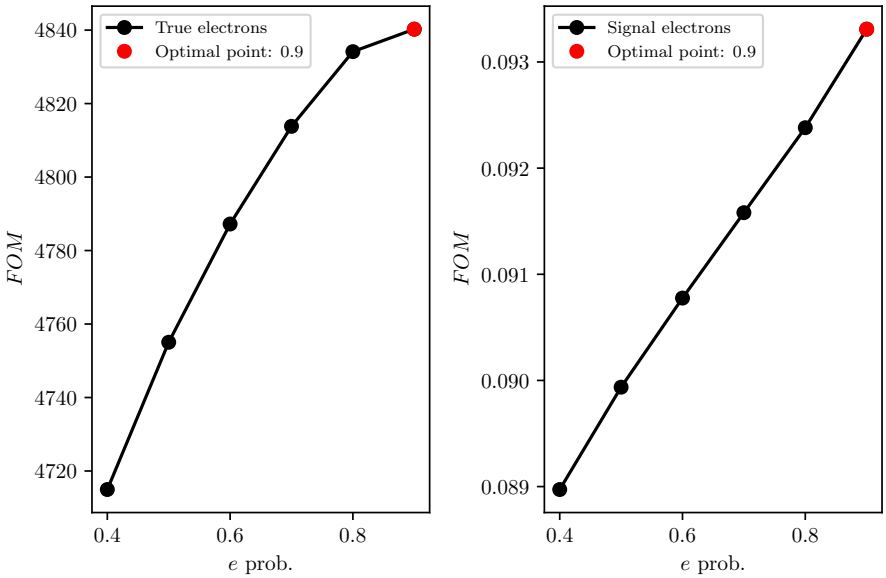

Figure 3.3: FOM optimizations of the PID probability cuts for true electrons (left) and true electrons from signal decays (right).

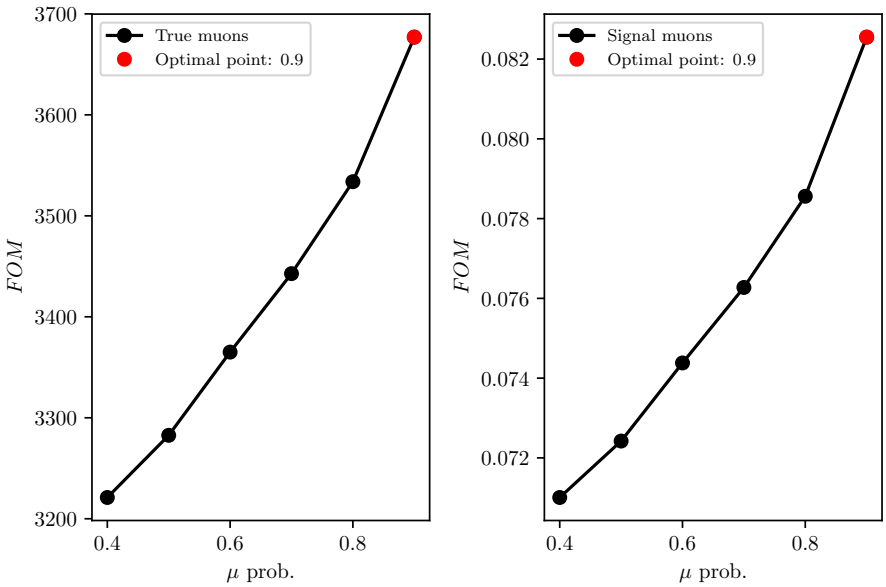

Figure 3.4: FOM optimizations of the PID probability cuts for true muons (left) and true muons from signal decays (right).

The optimized PID cuts for leptons are

- e prob. > 0.9 for electrons,
- μ prob. > 0.9 for muons.

The optimal value for the PID cuts is the same for all true leptons, if they are coming from signal decays or not, so this cut can be widely used on leptons coming from either B meson in our analysis.

Kaons

For the case of kaons, the procedure is the same and the cuts are very similar. Figure 3.5 shows the impact parameters d_0 and z_0, the momentum in $\Upsilon(4S)$ center-of-mass system (CMS), and the PID information for true and fake kaons, where an extra category for true kaons from the signal decay is shown.

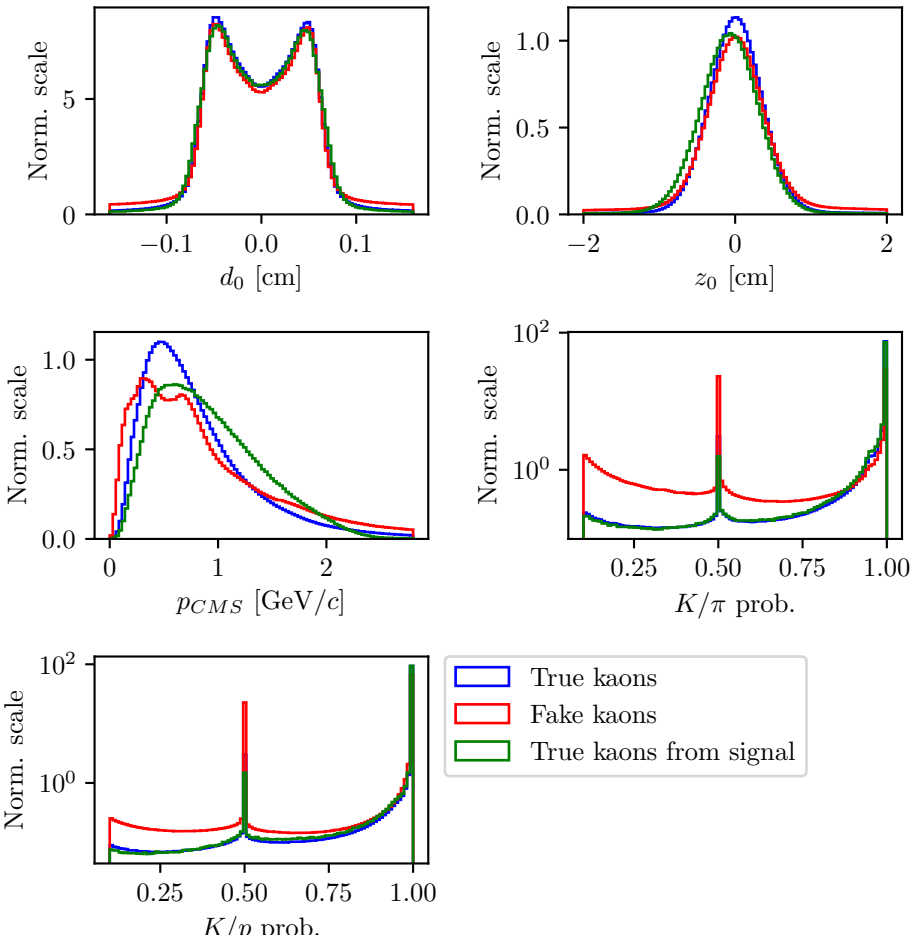

Figure 3.5: Normalized properties of true (blue), fake (red) and true kaons (green) from signal decay

.

We define the kaon cuts in the same manner as in the case for leptons

- $|d_0| < 0.15$ cm,
- $|z_0| < 1.5$ cm,
- $p_{CMS} \in [0,\ 2.5]$ GeV/c.

The PID optimization in this case is taken in two steps. First we optimize the cut on K/π, and after that the K/p separation probability. Figure 3.6 shows the optimization procedure for PID cuts on kaon candidates.

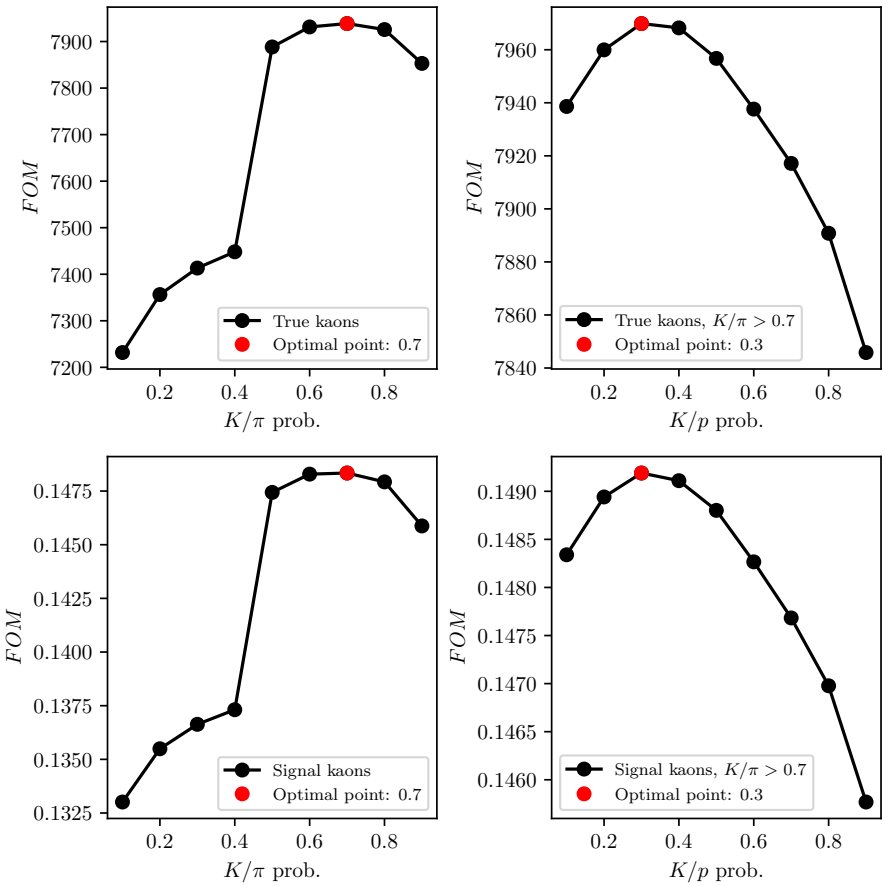

Figure 3.6: *FOM* optimizations of the PID probability cuts for true kaons (top) and true kaons from signal decays (bottom). The plots on the left show the optimization of the first step for the K/π probability cut, and the plot on the right the K/p probability cut.

The optimized PID cuts for kaons are

- $K/\pi > 0.7$,
- $K/p > 0.3$.

3.2 Combination of FSP particles

With the pre-selected kaon and lepton candidates we make appropriate combinations for potential B^+ meson candidates. Due to our inability to reconstruct the neutrino, we are only able, at this point, to reconstruct the B mesons in the following two channels

$$B^+ \to K^+K^-e^+,$$
$$B^+ \to K^+K^-\mu^+,$$

and similarly for B^-. In order to further guarantee the proper combination of FSP particles, we perform a vertex fit of the three tracks. B mesons have a relatively long lifetime, so they travel and decay along the z-axis of the detector in the direction of the boost, so we perform the vertex fit with an *iptube* constraint, which constrains the vertex to an elongated ellipsoid along beam direction. We demand that the fit converged and apply a cut on the fit probability. The fit probability for signal and background B meson candidates is shown in Figure X. We perform a FOM cut optimization of this variable, which is shown in Figure X.

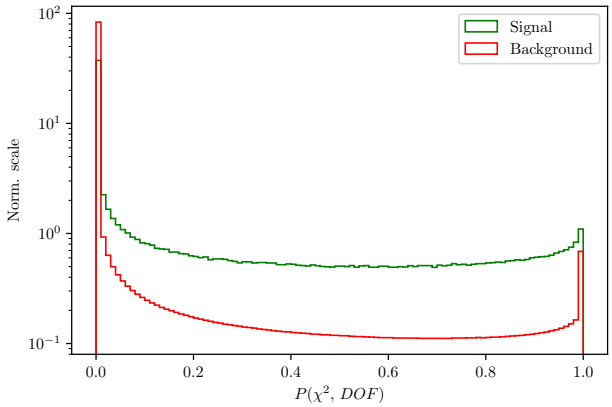

Figure 3.7: Normalized vertex fit probability distribution for signal and background B meson candidates in logarithmic scale.

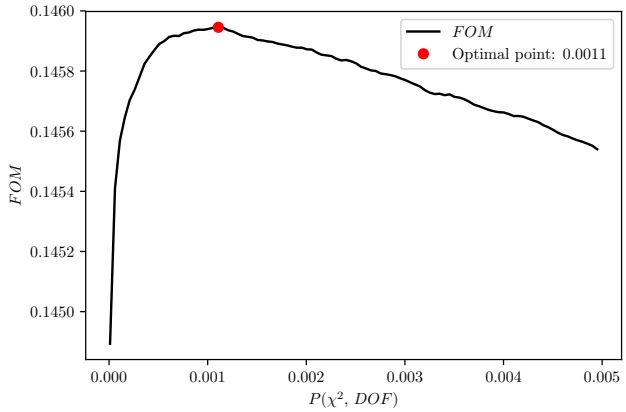

Figure 3.8: FOM optimization of the vertex fit probability.

The resulting PID cuts are then

- $P(\chi^2, NDF) > 1 \times 10^{-3}$.

With the neutrino being the only missing particle on the reconstructed side, it is possible to determine the angle between the direction of the reconstructed B (denoted as $Y \to KK\ell$) and the true B, as

$$\mathrm{p}_\nu = \mathrm{p}_B - \mathrm{p}_Y, \tag{3.2}$$

$$\mathrm{p}_\nu^2 = m_\nu^2 = m_B^2 + m_Y^2 - 2E_B E_Y + 2\vec{p}_B \cdot \vec{p}_Y \approx 0, \tag{3.3}$$

$$\cos(\theta_{BY}) = \frac{2E_B E_Y - m_B^2 - m_Y^2}{2|\vec{p}_B||\vec{p}_Y|}, \tag{3.4}$$

where all the energy and momenta above are calculated in the CMS frame. The mass of the neutrino equals to 0 to a very good precision, so we used it in Eq. (3.3). In addition, we can substitute the unknown energy and momentum magnitude, E_B and $|\vec{p}_B|$, of the B meson in Eq. (3.4), with quantities from the well known initial conditions

$$E_B = E_{CMS}/2, \tag{3.5}$$

$$|\vec{p}_B| = p_B = \sqrt{E_B^2 - m_B^2}, \tag{3.6}$$

where E_{CMS} is the total energy of the e^+e^- collision in the CMS frame and m_B is the nominal mass of the B meson.

For the correctly reconstructed candidates, this variable lies in the $[-1, 1]$ region, though only to a certain precision, due to the finite detector resolution. For background candidates, however, the values populate also the non-physical regions, as is shown in Figure

3.9. We impose an optimized cut on this variable from Figure 3.10 to discard a large amount of background.

- $|\cos(\theta_{BY})| < 1.0$.

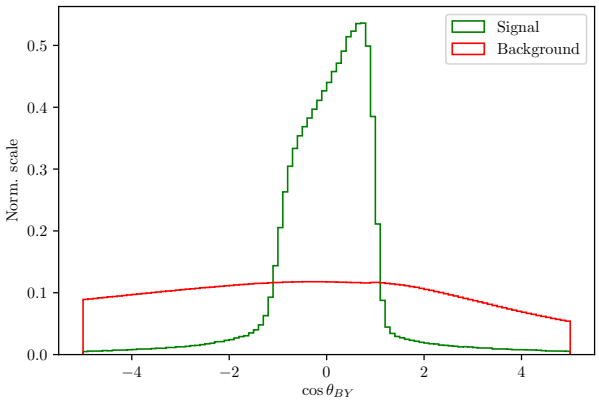

Figure 3.9: Normalized $\cos\theta_{BY}$ distribution for signal and background B meson candidates.

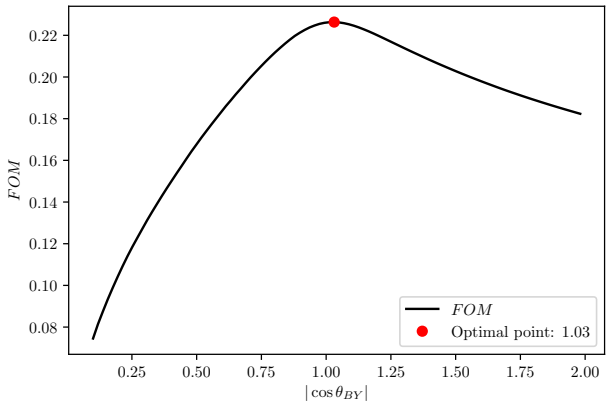

Figure 3.10: FOM optimization of the $\cos\theta_{BY}$ variable.

3.3 Rest of event clean-up

Due to the beam background in the detector, material interactions, or other processes, random tracks and clusters enter our event and get reconstructed as part of the physics process we want to study. These tracks and clusters are not interesting and further spoil

the data we measure. In order to remedy this, we perform an extensive clean-up of the tracks and clusters in the ROE side, before calculating the four-momentum of the missing neutrino. The clean-up procedure is performed separately on tracks and clusters and uses multiple steps with multivariate analysis (MVA) algorithms in order to separate good tracks and clusters from the bad ones, which populate the ROE. Then, for each ROE object, a ROE mask is created for tracks and clusters, which is used to narrate the use of this track or cluster in the final calculations of the ROE four-momentum.

In order to preserve the continuity of this chapter, a more detailed description of the ROE clean-up can be found in Chapter 4. From this point on in this chapter the reader can assume the ROE to be clean.

3.4 Loose neutrino reconstruction

The signal-side neutrino escapes detection, so we cannot directly determine it's four-momentum. However, due to the detectors geometry, which almost completely covers the full solid angle, and due to well known initial conditions of the $\Upsilon(4S)$ meson, it is possible to determine the kinematics of the missing neutrino via indirectly reconstructing the other B meson by summing up all the FSP particles four-momenta in the ROE. This is known as the *untagged* method. Here we see the motivation for the ROE clean-up. If we did not depend on the other B meson for our signal candidate reconstruction, this would not have been an issue.

The total missing four-momentum in the event can be determined as

$$\mathrm{p}_{miss} = \mathrm{p}_{\Upsilon(4S)} - \sum_{i}^{\text{Event}} (E_i, \vec{p}_i)\,, \tag{3.7}$$

$$\mathrm{p}_{miss} = \mathrm{p}_{\Upsilon(4S)} - \left(\mathrm{p}_Y - \sum_{i}^{\text{Rest of event}} (E_i, \vec{p}_i) \right). \tag{3.8}$$

where the summation runs over all charged and neutral particles in the defined set. We define the square of the missing mass, m^2_{miss}, which is zero, if signal side neutrino is the only missing particle in the event, as shown in Equation (3.10).

$$\mathrm{p}_\nu = \mathrm{p}_{miss} = (E_{miss}, \vec{p}_{miss})\,, \tag{3.9}$$

$$m^2_{miss} = \mathrm{p}^2_{miss} = \mathrm{p}^2_\nu = m^2_\nu \approx 0. \tag{3.10}$$

Since the detector is not perfect, the distribution of the m^2_{miss} variable has a non-zero width. Additionally, tails are introduced as soon as we have additional missing particles such as extra missing neutrinos or other neutral undetected particles such as

K_L^0, or simply missing tracks due to detection failure. Figure X shows the distribution of m^2_{miss} as defined with the missing four-momentum in Eq. (3.9). Correctly reconstructed candidates, which come from events where the other B meson decayed via a hadronic decay mode, should peak at zero. If this is not the case, candidates are shifted to larger values of this variable. Due to this fact, we impose a cut on the m^2_{miss} variable in order to discard all candidates with spoiled properties, even if it was in principle a correct combination of FSP particles on the signal side.

PLOT

The main uncertainty in neutrino four-momentum, defined as in Eq. (3.9) comes from energy uncertainty. It is a common practice to substitute the missing energy with the magnitude of the missing momentum, since the momentum resolution is much better, thus redefining the neutrino four-momentum to

$$\mathrm{p}_\nu = (|\vec{p}_{miss}|, \vec{p}_{miss})\,. \tag{3.11}$$

With our newly defined neutrino four-momentum, we can add it to the four-momentum of the $Y(KK\ell)$ candidate to obtain the full B meson four-momentum and calculate the traditional M_{BC} and ΔE variables

$$\Delta E = E_B - E_{CMS}/2, \tag{3.12}$$

$$M_{BC} = \sqrt{(E_{CMS}/2)^2 - p_B^2}. \tag{3.13}$$

Since the final fit will be performed on these two variables, we define two regions that will be used

- Fit region: $M_{BC} \in [5.1,\, 5.3]$ GeV/c^2 and $\Delta E \in [-1,\, 1]$ GeV,
- Signal enhanced region: $M_{BC} \in [5.X,\, 5.3]$ GeV/c^2 and $\Delta E \in [-X,\, X]$ GeV.

PLOT

3.5 q^2 calculation

4 Rest of event clean-up

Continuing from Section 3.3, the description of the ROE clean-up process is described here.

4.1 Setting up the MVA

Training the MVA classifiers follows the same recipe for all the steps. For each step we run our B meson reconstruction on Signal MC with a generic companion B meson. This way the produced weight files are less likely to be dependent on the signal side and can be used also for untagged analyses of other decays. For every correctly reconstructed signal B meson we save the necessary information for each MVA step (i.e. properties of ROE clusters). Only correctly reconstructed candidates are chosen here, to prevent leakage of information from the signal side to the ROE side.

For each cleanup-step a dataset of $2 \times N$ was prepared for the training of "signal" against "background". The dataset for each case was split into 5 parts for reasons which are explained later on in the note. The Fast-BDT (FBDT) [] algorithm was used as the MVA method, where the following hyper-parameters were optimized with a grid search

- `nTrees`: the number of trees in the FBDT forest,
- `nLevels`: the number of levels in each FBDT tree.

Figure X shows a graphical interpretation of the FBDT forest with `nTrees` and `nLevels`. In all cases the hyper-parameters were optimized with a grid search in the hyper-parameter space. Additionally, we perform a k-fold cross-validation ($k = 5$) for each hyper-parameter set, where we cycle through the 5 parts of the dataset and 4 parts of the dataset are used for training, whereas the remaining part is used for validation. This minimizes the bias towards the validation sample when optimizing the hyper-parameters. Figure X shows a schematic procedure of a k-fold cross-validation.

4.2 Clusters clean-up

Generally speaking, most of the photons in B-physics should come from $\pi^0 \to \gamma\gamma$ decays. However, a lot of clusters are also created by photons coming from the beam background or interactions with the detector material. These photons add extra energy and momentum which we then measure.

In the first step of the clusters clean-up we train an MVA which recognizes good π^0 candidates. The output of this classifier is then applied to photons and represents a sort of a π^0 probability, which is used as an additional classifier variable in the next step of the clean-up, where we train an MVA to separate good photon clusters from bad ones.

4.2.1 π^0 MVA training

The dataset of π^0 candidates contains

- 387125 signal candidates,
- 416019 background candidates,

where the definition of signal is that both photon daughters that were used in the reconstruction of the π^0 are actual photons and actual daughters of the particle, based on the MC truth. We use π^0 candidates from the converted π^0 particle list from Belle MC with the invariant mass in the range of $M \in [0.10,\ 0.16]$ GeV and perform a mass-constrained fit on all candidates, keeping only the cases where the fit converged.

The input variables used in this MVA are

- p and p_{CMS} of π^0 and γ daughters,
- $P(\chi^2, NDF)$ of the mass-constrained fit, invariant mass and significance of mass before and after the fit,
- angle between the daughter photons in CMS frame,
- cluster quantities for each daughter photon
  - $E_9/E25$,
  - theta angle,
  - number of hit cells in the ECL,
  - highest energy in cell,

  - energy error,
  - distance to closest track at ECL radius.

The classifier output variable is shown in Figure X.

PLOT

The distributions for all input variables and their correlations for signal and background candidates can be found in Appendix X for all steps of the clean-up.

4.2.2 γ MVA training

The dataset of γ candidates contains

- 324781 signal candidates,
- 333353 background candidates,

where the definition of signal is that the photon is an actual photon and that the related ECL cluster is related to a primary MC particle. This tags all photon particles from secondary interactions as background photons. We use γ candidates from the converted γ particle list from Belle MC. The π^0 probability information from the previous step is applied to all photon pairs which pass the same π^0 cuts as defined in the previous step. Since it's possible to have overlapping pairs, the π^0 probability is overwritten, if the new value is greater than the existing one, since this points to a greater probability of a correct π^0 combination.

The input variables used in this MVA are

- p and p_{CMS} of γ candidates,
- π^0 probability,
- cluster quantities
  - $E_9/E25$,
  - theta angle,
  - number of hit cells in the ECL,
  - highest energy in cell,

– energy error,

– distance to closest track at ECL radius.

The classifier output variable is shown in Figure X.

PLOT

4.2.3 Clusters clean-up optimization

We now have the final weights for photon classification. We apply these weights to the photon particle list, coming from the generically decaying B mesons with correctly reconstructed signal B mesons on the other side. After applying the weights we optimize the cut based on the standard definition of the FOM. The cut optimization is shown in Figure X, with the optimal cut on the γ classifier output at X.

PLOT

Figure shows the LAB frame momentum of the photons before and after the cut in logarithmic scale. The signal efficiency and background rejection at this cut are

- Signal efficiency: $\epsilon_{SIG} = X$,
- Background rejection: $1 - \epsilon_{BKG} = X$.

PLOT

4.3 Tracks clean-up

4.4 Selection after clean-up